

## Thermal conductivity of solid neon\*

J. E. Clemans<sup>†</sup>

Department of Physics and Materials Research Laboratory, University of Illinois, Urbana, Illinois 61801

(Received 3 November 1975)

The thermal conductivity of solid neon samples was measured from 0.5 to 10 K. An isotopically purified <sup>20</sup>Ne sample and a <sup>20</sup>Ne sample with 0.15-at.% <sup>4</sup>He, as well as a sample with the natural isotopic mixture, were studied. Measurements were made at molar volumes between 13.4 and 12.89 cm<sup>3</sup>/mole. The conductivity is found to increase rapidly with decreasing molar volume. The conductivity is determined primarily by the intrinsic phonon scattering above about 4 K. Normal and Umklapp phonon scattering terms are found to be necessary to make reasonable fits to the data using the Callaway relaxation-rate theory. The functional form of the three-phonon Normal processes can be represented best by  $\tau_N^{-1} \propto B_N x^2 T^4 \text{ sec}^{-1}$ , where  $x = \hbar\omega/kT$ ,  $\omega$  is the phonon frequency, and  $B_N$  is a constant. These fits show that the enhancement of phonon scattering from isotopic defects due to differences in zero-point energy decreases with molar volume.

### I. INTRODUCTION

The theoretical evaluation of the lattice thermal conductivity of any insulating solid whose interatomic potential is known was originally outlined by Leibfried and Schlömann<sup>1</sup> in a form known as the "Ziman limit".<sup>2</sup> Very few calculations based on this theory have been carried out, because a good theoretical model of the anharmonic interatomic forces in the material must be available. This is the case in a few alkali halide and noble-gas solids. Calculations employing this fundamental point of departure have been made for NaF and LiF.<sup>3</sup> The application of this approach to helium is difficult because sophisticated descriptions of the interatomic interaction required to take into account large "quantum" effects have not been developed. The theory has been applied to the heavier rare-gas solids. Fairly simple calculations accurately predict the conductivity of krypton.<sup>4-6</sup> These calculations are somewhat less accurate for argon,<sup>4-6</sup> and more sophisticated modifications of the potentials<sup>7</sup> and methods<sup>8</sup> have been employed. So far, attempts to calculate the thermal conductivity of neon have given the least accurate predictions of all. This difficulty is not unexpected, since neon is lighter and exhibits larger quantum-mechanical effects. However, in comparison with helium, this effect is modest enough that it may prove possible to calculate by conventional two-body methods.

These calculations are carried out in the Ziman limit using the Lennard-Jones (6-12) interatomic potential. They employ phonons resulting from either the classical harmonic approximation,<sup>4,6</sup> or a self-consistent harmonic approximation which incorporates zero-point effects.<sup>5</sup> These calculations for perfect infinite crystals are shown graphically in Fig. 1. Benin<sup>5</sup> discussed the fundamen-

tal problems associated with the simple Planck phonon distributions employed in this limit. However, he comments that the apparent discrepancies between the calculations and the data of White and Woods<sup>9</sup> are obscured by uncertainties in the parameters of the interatomic potential.

One impediment to further theoretical work has been the dearth of experimental thermal conduc-

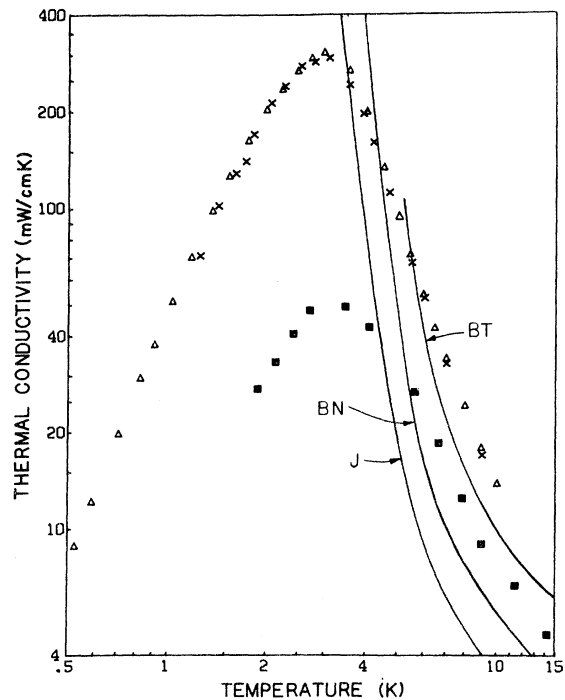


FIG. 1. Thermal conductivity of isotopically purified <sup>20</sup>Ne and "Ziman limit" theoretical results.  $\Delta$ , sample 18 from present work;  $\times$ , Kimber and Rogers (1973);  $\blacksquare$ , natural neon White and Woods (1958). Theoretical curves: (J), Julian (1965); (BN), Benin (1968); (BT), Bennett (1970).

tivity data, which has been limited in quality by extensive mechanical damage in the samples of White and Woods.<sup>9</sup> Data on better samples has been needed to provide thermal conductivity values that more closely reflect the intrinsic, rather than defect, scattering processes of neon. In addition, measurements at constant volume are especially useful, since the lattice constant plays an important role in fundamental calculations. The experiment described here was initiated to improve the sample quality, and much higher quality samples were indeed obtained. Thermal conductivities are reported here for samples of various molar volumes and isotropic concentrations from 0.5 to 10 K. Data at various molar volumes provide a more stringent test of the theoretical calculations, because quantum effects decrease in importance as the molar volume decreases.

While this experiment was in progress, Kimber and Rogers reported thermal conductivity data for solid neon<sup>10</sup> (hereafter referred to as KR). Their samples were grown at the molar volume given by the vapor-pressure curve, using various isotopic concentrations. There is substantial agreement between the data of KR and the part of the present data which was taken under similar conditions.

Section II describes the experimental equipment and procedures used in sample growth and measurement. Section III describes the results of these measurements and discusses computer fits of various phenomenological expressions to the data.

## II. EXPERIMENTAL METHOD

The measurement of the thermal conductivity of solid neon at constant volume requires crystal growth at high pressure and cryostat which can operate efficiently between 0.5 and 50 K. In this investigation, cylindrical neon samples were grown *in situ* under constant pressures of up to 1750 bars. Typical solidification temperatures were 45 K, compared with the melting point at vapor pressure of 24.5 K. After growth at pressures above 700 bars, the solid could be maintained at constant volume while conductivity measurements were made from 10 to 0.5 K. The sample chamber was clamped onto a heat sink in an evacuated can which was immersed in liquid helium. The heat sink was equipped with a <sup>3</sup>He pot for work below 1.2 K. This section describes the special experimental equipment and techniques used to carry out this investigation.

### A. Apparatus

A system that used a total gas volume of only 5 STP liters was developed for thermally generating

and controlling 2000 bar pressures of neon. The pressure system is presented schematically in Fig. 2. The sample gas is purified by cryopumping it through a heated titanium getter and a liquid-nitrogen cold trap. This operation charges the pressure generating cell (PGC) with solid neon at 4.2 K. Very effective removal of helium impurity atoms was achieved by vacuum pumping on the vapor over the solidified neon in the PGC. High-pressure neon gas was generated by heating the PGC to about 200 K. An unusual feature of this system was the use of strain gauges for dynamic pressure control, which was better than 0.01% during the growth of a sample. The gauges were mounted on a small volume element outside the cryostat. Electronic feedback from the gauges controlled the heating of the PGC.

The sample chamber (Fig. 3) was made from 316 stainless steel tubing. The outer and inner diameters were 0.318 and 0.152 cm, respectively. Three 0.013-cm-thick copper disks were brazed to the tube with 1.00-cm spacings between the upper edges of adjacent disks. The disks were preformed with a mandrel to have a ledge, on which a 1000- $\Omega$  heater was wound. The disks mark off the upper and lower sections of the sample across which the thermal conductivity is measured (as will be discussed below). Mounts are provided for two germanium thermometers at both top and bottom of the sample chamber.

### B. Sample growth

A general procedure for the growth of solid neon crystals evolved during the growth of over 80 sam-

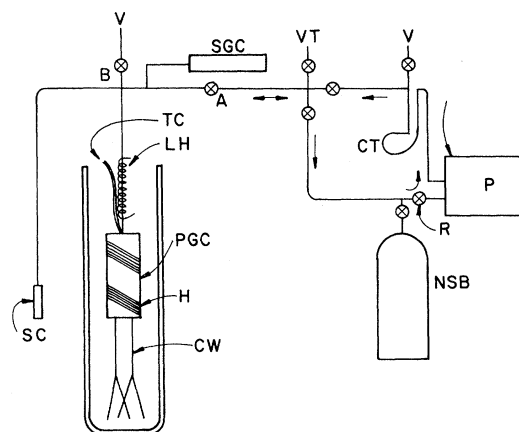


FIG. 2. Pressure System: CT, nitrogen cold trap; CW, No. 14 copper wire; H, heater; LH, line heater; NSB, neon storage bottle; P, purifier (heated titanium); PGC, pressure generating cell (3 cm<sup>3</sup>); R, gas regulator; SC, sample chamber (0.2 cm<sup>3</sup>); SGC, strain-gauge pressure sensing cell; TC, thermocouple; V, vacuum port; VT, vent.

ples. Only 18 of the samples were selected for complete thermal conductivity measurements. Before beginning the discussion of growth techniques, we note that ten of the measured samples (1-10) had the "natural" isotopic mixture (9.27-at.%  $^{22}\text{Ne}$  and 0.027-at.%  $^{21}\text{Ne}$  in  $^{20}\text{Ne}$ ). Isotopically "pure" neon with 0.012-at.%  $^{22}\text{Ne}$  and 0.039-at.%  $^{21}\text{Ne}$  in  $^{20}\text{Ne}$  is used in the remaining eight crystals (11-18) three of which (11-13) were contaminated with 0.15-at.%  $^4\text{He}$ . These impurity concentrations were obtained from mass spectroscopic analysis. Impurities other than those mentioned were not present at 0.001 at.%, the minimum detectable concentration.

Solidification begins at the tail of the sample chamber, which is controlled at  $T = T_m(P) - \delta T$ . Here  $T_m(P)$  is the melting temperature at the growth pressure  $P$ , and  $\delta T$  represents the amount of undercooling of the tail. The solid-fluid interface moves up the sample tube and out the inlet as the temperature of the copper heat sink is lowered. The pressurization system pumps neon into the

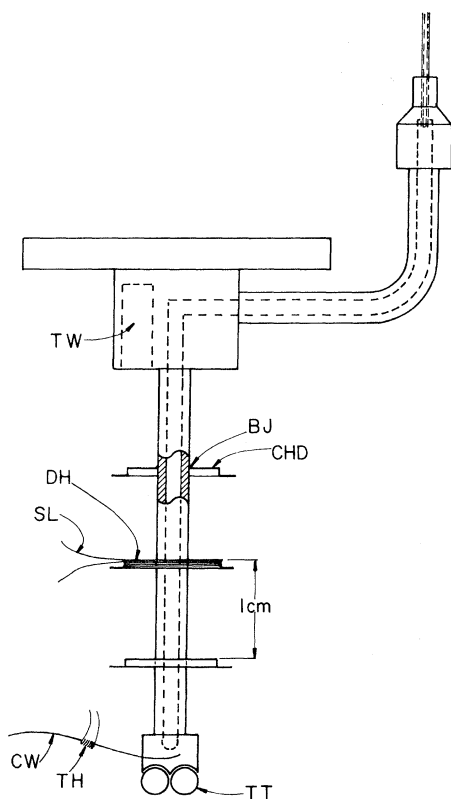


FIG. 3. Sample Chamber: BJ, brazed joint; CHD, copper heating disk (0.013 cm thick); CW, No. 24 copper wire which leads to the heat switch; DH, disk heater (1000  $\Omega$ ); SL, superconducting lead; TH, tail heater; TT, germanium thermometer; TW, one of two wells for the control thermometers.

sample chamber to maintain the pressure. The inlet heater is turned off when the entire sample volume is at  $T = T_m - \delta T$ . The neon freezes in the inlet tube, sealing the sample at constant volume for the remainder of the experiment. Next, the mechanical switch which cools the tail of the sample chamber (by clamping on the wire "CW" in Fig. 3, connecting it to the  $^4\text{He}$  bath) is disconnected. Cooling is then started if it is not already in progress. The crystal is cooled at 2 K/h. This keeps the temperature gradient along the sample below 0.06 K/cm. After several hours, the heaters are turned off and the system relaxes from about 20 to 4 K. The maximum temperature gradient is less than 0.35 K/cm.

Faster cooldown rates produced samples with lower conductivities. Many natural neon samples were rejected because they had conductivities which were depressed by some approximately constant multiplicative factor from those of the best crystals. KR report such reductions in the conductivity of thermally shocked samples. A different type of damage was observed in "pure"  $^{20}\text{Ne}$  samples. Their conductivities showed a very sharp limit to the phonon mean free path below 4 K. See sample 17 on Fig. 4. The only sample (18) that did not show this behavior was cooled very slowly and evenly (the largest temperature gradient was less than 0.1 K/cm). See Fig. 4.

The size of  $\delta T$ , the undercooling of the tail, was an important growth parameter. Under a variety

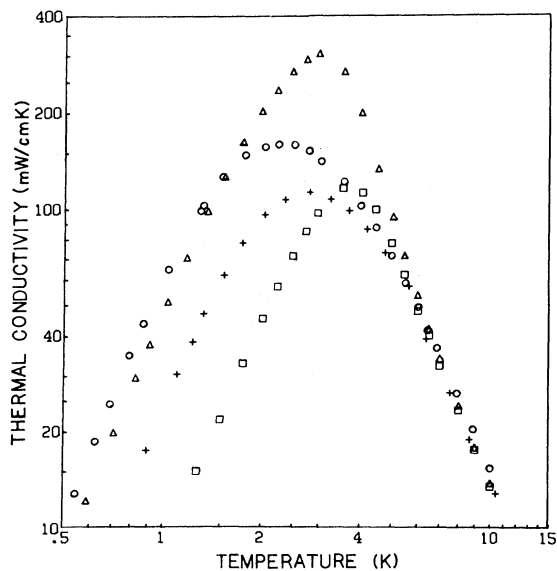


FIG. 4. Isotope effect on thermal conductivity. All molar volumes are approximately  $13.4 \text{ cm}^3/\text{mole}$ .  $\circ$ , sample 3; and  $+$ , Kimber and Rogers (1973), natural neon;  $\square$ , sample 17; and  $\Delta$ , sample 18, isotopically "pure" neon.

of annealing conditions, large  $\delta T$ 's of 7 to 10 K resulted in mechanically damaged samples. A sample with  $\delta T=0.6$  K had less damage. Sample 10, with  $\delta T\sim 0.0$  K was the best natural neon sample grown. Similar effects of  $\delta T$  were observed in isotopically pure samples with 0.15-at.%  $^4\text{He}$  impurities.

The molar volume of sample 10 was inferred from its melting temperature  $T_m=42.7$  K. By extrapolating data on an isochore of neon<sup>11</sup> to the melting curve, we find a corresponding molar volume of  $12.89\pm .01$  cm<sup>3</sup>/mole. Similarly, the data for sample 13 are:  $T_m=43.96$  K and  $V=12.82$  cm<sup>3</sup>/mole. [However, the high-temperature conductivity of sample 13 is below that of sample 10, opposite what we expect from the smaller molar volume. We suspect that it has suffered an (undetected) thermal shock of the type discussed by KR.] In sample 18, a definite  $T_m$  could not be found.  $T_m$  was 30.96 K for sample 17, which allows thermal expansion below 10 K. Now, the high-temperature data from sample 17 agrees (in Fig. 4) with that of sample 18, which in turn coincides with the data for the freely expanding sample of KR (in Fig. 1). Thus, samples 17 and 18 may be said to have the free expansion molar volume (at 0 K) of 13.4 cm<sup>3</sup>/mole. The conductivity of sample 3 at 6 K (below the temperatures where thermal expansion is important) agrees with those of KR natural neon samples. See Fig. 5.

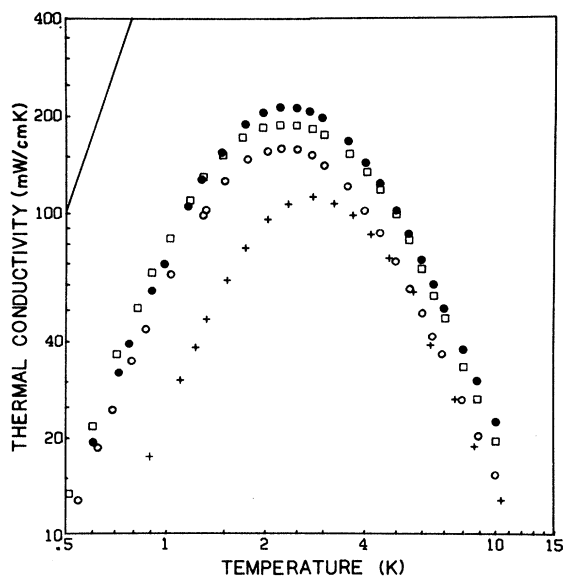


FIG. 5. Thermal conductivity of natural neon samples:  $\circ$ , sample 3; and  $+$ , Kimber and Rogers (1973), both with molar volume 13.4 cm<sup>3</sup>/mole;  $\bullet$ , sample 10 at 12.89 cm<sup>3</sup>/mole. Also shown is  $\square$ , sample 13, which is pure  $^{20}\text{Ne}$  with 0.15-at.%  $^4\text{He}$  and a molar volume of 12.82 cm<sup>3</sup>/mole.

The conductivity of sample 3 has the same dependence between 6 and 10 K as sample 10, indicating that it has remained at constant volume during measurement. Because  $T_m$  was not measured for this sample, its molar volume cannot be positively established. In the light of the agreement with the KR samples at 6 K we assign it the molar volume 13.4 cm<sup>3</sup>/mole, on the assumption that thermal shock has not affected its conductivity.

### C. Thermal conductivity measurements

The thermal conductivity of neon in the two 1-cm sections of the sample chamber between the copper disks (Fig. 3) was calculated from the measured heat current, temperature gradient, and geometrical factors. During conductivity measurements, one thermometer controlled the temperature of the copper heat sink. The other thermometer measured the temperature of the tail of the sample chamber. Identical powers  $P$  were dissipated successively on each of the three tail heating disks. In equilibrium, this produced three different temperatures  $T_i$  at the measurement thermometer. When the power is dissipated on disks at either end of section " $i$ ,"  $\Delta T_i = T_{i+1} - T_i$  gives the temperature gradient created by the heat current  $P$  through that section. The thermal conductivity was then calculated for each section, after taking into account the fraction of the power which was transmitted through the stainless steel walls of the sample chamber. Measurements on two sections of the neon sample provided a consistency check on the data. In some instances, differences in the molar volume or mechanical damage of the two sections were detected.

Estimates of the experimental errors in  $\kappa$  are 4.5, 1.1, and 3.0% at 0.5, 2.5, and 8 K, respectively. For some samples, the accuracy of the measurements of  $\kappa$  is undermined by the uncertainty in the molar volume. In several samples, the differences in the experimental value of  $\kappa$  between the sections of the same sample exceed the error in  $\kappa$ , indicating the presence of density gradients. A 5% uncertainty is added to  $\kappa$  from an uncertainty of 0.4% in the molar volume.

## III. RESULTS AND ANALYSIS

### A. Results

The measured values of the thermal conductivity of isotopically purified  $^{20}\text{Ne}$  give the clearest representation of the intrinsic phonon scattering. Figure 1 compares data from the present work with recent data of KR on a sample of similar purity. The agreement here is well within the experimental error in the 4–10-K range. This

agreement experimentally establishes the value of thermal conductivity in the temperature region where intrinsic phonon scattering is dominant. The concave upward curvature of the conductivity in this range is a result of the fact that the intrinsic Umklapp scattering, which is proportional to  $e^{-\Theta/aT}$ , is a more important process than the competing defect scattering. This same feature dominates the various theoretical estimates of the thermal conductivity shown in Fig. 1. Sample 18 probably undergoes thermal expansion above 6 K, as do all the samples of KR. The effect of the varying molar volume on the conductivity is discussed further below. Defect scattering takes over rapidly at low temperatures indicating mechanical defect concentrations close to those for natural neon samples.

Thermal conductivity measurements were made on a natural neon crystal with a molar volume approximately the same as those of KR. The agreement in the temperature range above the thermal conductivity maximum, between this sample and those of KR is shown in Fig. 5, and will be discussed in detail below. This figure also shows that at low temperatures the thermal conductivity of the samples from the present work are several times higher than the highest value of KR. Since in this low-temperature region, phonon scattering is primarily dominated by scattering from dislocations, the results show these defects to be two to three times less dense than in the KR samples.

The conductivity of the natural neon sample 10, with molar volume  $12.89 \text{ cm}^3/\text{mole}$ , is also shown in Fig. 5. This is compared with a  $^{20}\text{Ne}$  sample contaminated with 0.15-at. %  $^4\text{He}$ .

A comparison of the neon thermal conductivity data from isotopically pure samples and those with the natural isotopic mixture is made in Fig. 4. The major differences between sample 18 and sample 3 is the 9.27-at. % concentration of  $^{22}\text{Ne}$  which exists as a mass defect in natural neon and scatters phonons strongly in the region of the peak thermal conductivity.

At the highest temperatures the thermal conductivity of the pure samples falls 10% below that of natural neon. See Fig. 4. A similar deviation exists between the natural neon data of the present work and that of KR, as shown in Fig. 5. The maximum error in the conductivity is not large enough to account for the discrepancy.

It has been shown<sup>7,12</sup> that thermal conductivity data for argon at temperatures well above the conductivity maximum deviate into two branches. Argon data from samples which have been allowed to expand freely<sup>13</sup> have conductivities well below those of samples held at constant volume.<sup>12</sup> We may estimate the size of such a conductivity affect for

neon. The thermal expansion in neon<sup>14</sup> at 10 K gives  $V(10 \text{ K})/V(0 \text{ K}) = 1.005$ . Data from the present experiment shows the strong dependence of the thermal conductivity on molar volume (discussed in Sec. III B). From this dependence, we expect the conductivity to be about 5% lower for expanding neon than for the constant volume samples by the time the temperature has been raised to 10 K. Thus, the observed deviation can be accounted for within experimental error.

#### B. Callaway analysis

The fundamental theories for infinite perfect crystals assume that all thermal resistance is the result of Umklapp scattering. Any effect of a finite Normal process scattering rate, as well as contributions of extrinsic scattering due to crystal defects, is left out of calculations made in the Ziman limit. However, these resistive processes are present in the results reported here. To estimate the effects of different scattering mechanisms, Callaway's phenomenological relaxation time theory<sup>15</sup> may be applied. It sums the relaxation rates of various scattering processes into a total relaxation rate  $\tau_c^{-1}$ . The Callaway theory converts this rate into the relaxation time in an integral modification of the equation for the thermal conductivity of gases. However, in the temperature range of the present experiment, the physical complexities of three-phonon (intrinsic) scattering<sup>16</sup> make it impossible to find exact expressions for the relaxation rates, since the temperature and volume dependences of the various rates are expected to vary over this range.

The Callaway expression for the thermal conductivity is  $\kappa = \kappa_1 + \kappa_2$ , where  $\kappa_1$  would represent the conductivity if Normal process scattering were small, while  $\kappa_2$  is included when Normal processes are significant:

$$\kappa = \kappa_1 + \kappa_2,$$

where

$$\begin{aligned} \kappa_1 &= GT^3 \int_0^{\Theta/T} dx J_4'(x) \tau_c, \\ \kappa_2 &= GT^3 \left| \int_0^{\Theta/T} dx J_4'(x) \left( \frac{\tau_c}{\tau_N} \right) \right|^2 \\ &\quad \times \left[ \int_0^{\Theta/T} dx J_4'(x) \left( \frac{\tau_c}{\tau_N \tau_R} \right) \right]^{-1}, \end{aligned}$$

$G = k^4/\hbar^3 2\pi^2 v$ ,  $x = \hbar\omega/kT$ , and  $J_n'(x) = x^n e^x / (e^x - 1)^2$ . The combined relaxation rate obeys  $\tau_c^{-1} = \sum_i \tau_i^{-1}$ , where  $i$  ranges over the operative scattering processes. In this case, contributions to the total rate are made by boundary, dislocation, isotope, Normal, and Umklapp scattering processes.

when Normal process rates  $\tau_N^{-1}$  are omitted from  $\tau_c^{-1}$ , we have,  $\tau_R^{-1} = \sum_{i \neq N} \tau_i^{-1}$ . We note that when only the  $\kappa_1$  term is used to fit solid neon data (and  $\tau_N$  is included in  $\tau_c$ ), the parameters found for various scattering processes give values of  $\kappa_2 \sim \kappa_1$ . They give Normal and Umklapp scattering rates of comparable size. Thus, the full expression  $\kappa = \kappa_1 + \kappa_2$  must be used.

The general expression for  $\tau_c^{-1}$  used in computer calculations was, in cgs units,

$$\begin{aligned} \tau_c^{-1} &= \tau_B^{-1} + \tau_D^{-1} + \tau_I^{-1} + \tau_N^{-1} + \tau_U^{-1} \\ &= 2.014 \times 10^7 V^{-2.18} R^{-1} + 7.0 \times 10^{-4} N_d x T \\ &\quad + 4.75 \times 10^{-3} S V^{7.53} \Gamma_M x^4 T^4 + B_N x^2 T^4 \\ &\quad + B_U x^2 T^5 e^{-\Theta/6.5 T} . \end{aligned}$$

$R$  is the sample diameter,  $N_d$  the dislocation density, and  $\Gamma_M$  the mass defect  $\sum_i f_i (\Delta M_i / M)^2$ .  $S$  is the zero-point enhancement factor. The Debye temperature  $\Theta$  is proportional to  $V^{-\gamma}$ .  $\gamma$  equals 2.51.<sup>17</sup>  $B_N$  and  $B_U$  are adjustable parameters.

The determination of the frequency and temperature dependences of  $\tau_N^{-1}$  and  $\tau_U^{-1}$  is not a rigorous procedure.<sup>16,18-20</sup> At temperatures substantially below  $\Theta$ , the occupation of the energy state  $\frac{1}{2}k\Theta$ , half the zone-boundary energy in the Debye approximation, is proportional to  $e^{-\Theta/aT}$ . The theoretical value of  $a$  for fcc crystals is 2.3,<sup>18</sup> rather than the Debye value of 2. However, neutron scattering data<sup>21</sup> from neon at 700 bars shows that for transverse phonons in the  $\langle 111 \rangle$  direction,  $E_{ZB}/k = 36.3$  K, where  $E_{ZB}$  has the same volume dependence as  $\Theta$ . The corresponding  $\Theta(T=0, 700 \text{ bars})$  is 75.1 K. Thus, assuming  $E_{ZB\langle 111 \rangle}$  to be the minimum  $E_{ZB}$ , the value of  $a$  is given by  $2(k\Theta/E_{ZB}) = 4.1$ . Temperature and frequency dependences of the Umklapping phonons are roughly the same as those of the Normal process phonons.

The form

$$\tau_N^{-1} + \tau_U^{-1} = B_N x^2 T^4 + B_U x^2 T^5 e^{-\Theta/6.5 T}$$

for the intrinsic scattering relaxation rate allows a better fit to data than other temperature and frequency dependences tried.<sup>22</sup> KR used this same expression, except that they used 5.8 instead of 6.5. The values of  $B_N$  and  $B_U$  for this fit (to natural neon sample 3) are  $2.5 \times 10^5$  and  $0.97 \times 10^5 \text{ sec}^{-1} \text{ K}^{-5}$ , respectively, when  $S$  is 1.25. The over-all quality of the fit is impaired for choices of  $B_N$  outside the range  $4.5 \times 10^5 - 2.0 \times 10^5 \text{ sec}^{-1} \text{ K}^{-4}$ ; for  $B_U$  and  $S$  the corresponding ranges are  $1.1 \times 10^5 - 0.85 \times 10^5 \text{ sec}^{-1} \text{ K}^{-5}$  and 1.0-1.5, respectively. Fits to pure  $^{20}\text{Ne}$  (sample 18) using this form for  $\tau_N^{-1} + \tau_U^{-1}$  or various other forms were less accurate and the resulting values of  $B_N$  and  $B_U$  could not be used as

the starting point in fits to isotopically less pure samples.

An independent check on the values of  $B_N$  and  $B_U$  could be obtained from neutron scattering data where the temperature-dependent phonon relaxation time  $\Gamma$  equals  $(\tau_N^{-1} + \tau_U^{-1})^{-1}$ .<sup>18,23</sup> Leake *et al.*<sup>21</sup> set upper limits on this parameter of  $6.6 \times 10^{-12}$  sec for longitudinal phonons of frequency  $\omega = 26.1k/\hbar$  K at 25 K. To compare the values of  $B_N$  and  $B_U$  used here with this limit, the temperature dependences of  $\tau_N^{-1}$  and  $\tau_U^{-1}$  must be employed to extrapolate to 25 K from the region of interest here (i.e., 4-10 K). Direct extrapolation of the fitted values of  $B_N$  and  $B_U$  to 25 K at the frequency  $26.1k/\hbar$  K gives a value of  $\Gamma^{-1}$  that is almost 5 times larger than  $1.5 \times 10^{11} \text{ sec}^{-1}$ . However, the temperature dependence of the relaxation times should decrease with increasing temperature. This argument is supported by calculations of  $\Gamma$  made for solid argon by Jones.<sup>23</sup> His calculations show that the temperature dependence decreases rapidly above 16 K. Taking this effect into account, we predict that the values of  $B_N$  and  $B_U$  calculated here should be adjusted to give

$$(\tau_N^{-1} + \tau_U^{-1})_{T=25 \text{ K}}^{\omega=26.1(k/\hbar) \text{ K}} \leq 1.52 \times 10^{11} \text{ sec}^{-1} .$$

A more definitive test would be provided by experimental values of  $\Gamma$  from neutron scattering at a temperature in the 4-10-K range, especially at an energy of one-half  $E_{ZB}$  ( $\sim 18k$  K) in the  $\langle 111 \rangle$  direction.

The Callaway theory has not been generalized to include molar volume variations. The first-principles calculation of Leibfried and Schlömann<sup>1</sup> predicts the volume dependence in the temperature range  $T > \Theta$ ,  $\kappa(V) \propto a\Theta^3 \propto V^{-7.2}$ . In the low-temperature limit, it can be shown that  $\kappa(V) \propto V^{5.3}$ , by using the relation  $\kappa = 1/3CvR$ , and taking the specific heat and the sound velocity in the Debye approximation. The mean free path  $R$  is a constant at low temperatures where boundary scattering is dominant. The temperature range of the present experiment is between these limiting cases. The Callaway theory is used to achieve a first approximation to the strengths of the various scattering mechanisms. The molar volume dependence of fitted values of  $B_N$  and  $B_U$  are  $V^{15}$  and  $V^9$ , respectively, when expressed as powers of  $V$ . In view of the uncertainties in choosing proper Callaway forms, however, these powers have only order of magnitude accuracy. Empirically, comparing samples 3 and 10 in the 5-10-K range, we can write  $\kappa = 2500(T/K)^{-2.2} (V/13.4 \text{ cm}^3/\text{mole})^{-11 \pm 3} \text{ mW/cm K}$ .

The  $T^{-2.2}$  dependence is the result of the competition of intrinsic and extrinsic scattering processes

in these natural neon samples. It may be contrasted with the exponential dependence of the pure neon sample (18). If only Umklapp processes are considered, Peierls<sup>2,24</sup> predicted that the conductivity of a perfect insulator would vary according to the relation

$$\kappa = A(T/\Theta)^n e^{\Theta/aT},$$

where  $A$ ,  $a$ , and  $n$  depend on the details of the material. Figure 6 shows the conductivities of samples 3, 10, and 18 plotted as a function of  $\Theta/T$ . Lines with  $n=0$ ,  $a=4$ , and  $A_{10}=2.82$  mW/cm K, and  $A_{18}=2.32$  mW/cm K are fit to samples 10 and 18. The exponential fit is similar to results in <sup>4</sup>He.<sup>25</sup> The value of  $\kappa$  at the two highest temperature points shown for sample 18 are decreased due to thermal expansion. Data for higher values of  $\Theta/T$  show the effect on  $\kappa$  of extrinsic scattering.

The isotope scattering relaxation time<sup>26</sup> used in the Callaway fit is

$$\begin{aligned} \tau_I^{-1} &= S(a^3/4v^3)(k/\hbar)\Gamma_M x^4 T^4 \\ &= 4.75 \times 10^{-3} S V^{7.53} \Gamma_M x^4 T^4. \end{aligned}$$

This is essentially "Rayleigh" phonon scattering from the density variations due to the presence of isotopic defects. In the case of neon where the interatomic forces are weak and the isotopic mass differences are large, additional scattering results from force-constant changes and local strain fields

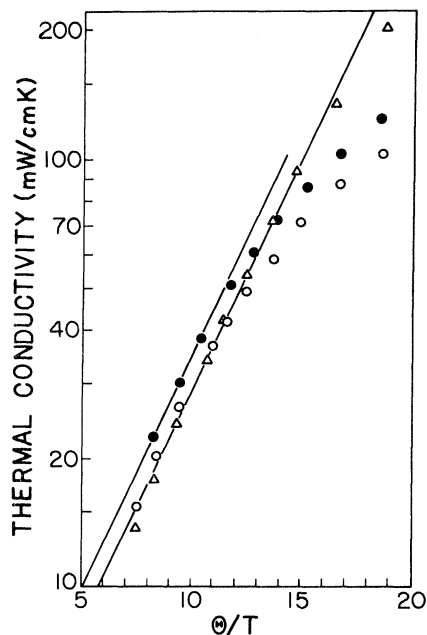


FIG. 6. Exponential temperature dependence of the conductivity in the Umklapp range. The straight lines obey  $\kappa = A(\Theta)e^{\Theta/4T}$ , with  $A(\theta)$  values listed in the text.  $\circ$ , sample 3; and  $\Delta$ , sample 18 have  $\Theta=75.1$  K;  $\bullet$ , sample 10 has  $\Theta=83.1$  K.

which disrupt the regularity of the lattice.<sup>27</sup> At low temperatures this perturbation is further aggravated by isotopic differences in zero-point motion.<sup>28,29</sup> The scattering enhancement is accounted for by the multiplicative factor  $S$ , which is a function of  $\Delta M/M$  and the relative change in force constants. For neon, an analysis by Jones<sup>28</sup> predicts  $S=1.4$ . The best value of  $S$  found in Callaway fits varied considerably  $1.25 \pm 0.25$ . It was strongly dependent on the form of  $\tau_N^{-1} + \tau_D^{-1}$  selected. More reliable estimates may be made of the ratio of  $S$  values between different samples, since the dependence on form is partially removed. For example,  $S$  values for natural neon samples 3 and 10 (at different molar volumes) give the result  $S(13.4 \text{ cm}^3/\text{mole})/S(12.89 \text{ cm}^3/\text{mole}) = 1.5 \pm 0.3$ . This indicates that the zero-point enhancement decreases with decreasing molar volume. This effect has been observed in solutions of <sup>3</sup>He-<sup>4</sup>He under more rigorous circumstances by various experimenters.<sup>30</sup> In a similar manner it is possible to compare the <sup>22</sup>Ne isotope scattering in sample 10 with the <sup>4</sup>He impurity scattering in sample 13. The small molar volume differences (discussed above) were ignored, and fits were made to sample 13 using a molar volume of 12.89 cm<sup>3</sup>/mole. In this calculation the mass of the <sup>4</sup>He impurity atom was inserted in the mass defect  $\Gamma_M$ . The value of the ratio  $S(^4\text{He})/S(^{22}\text{Ne})$  is approximately 2.

The relaxation rate for diffuse scattering of phonons from the boundaries of a crystal of diameter  $R$  is given by  $\tau_B^{-1} = v/R$ .<sup>31</sup> In the case of a polycrystalline sample,  $R$  represents an average grain size.<sup>32,33</sup> Since  $\tau_B^{-1}$  is temperature independent, the temperature dependence of the thermal conductivity is the same as that of the specific heat, i.e.,  $T^3$ . This scattering is dominant at very low temperatures when other relaxation processes are frozen out. In the present samples, dislocation scattering mechanisms are still important even at 0.5 K. The relaxation rate for dislocation scattering, derived from the interaction of phonons with the strain field of a static dislocation,<sup>18,26,34</sup> is  $\tau_D^{-1} = 7.0 \times 10^{-4} N_d x T$ . Below 1 K the temperature dependence of the thermal conductivity of sample 3 (and all of the samples reported here) is  $T^{2.7}$  or  $T^{2.6}$ . Over the limited temperature range of this experiment, parameters  $R$  and  $N_d$  may be found to balance the boundary and dislocation limits to  $\kappa$  which depend, respectively, on  $T^3$  and  $T^2$ . The  $R$  values found in all fits indicate average grain sizes of one-tenth the 1.5-mm sample diameter. If the thermal conductivity were only limited by boundary scattering, it would have the value sketched in Fig. 5. These values of  $R \sim 0.015$  cm indicate grain sizes 2-4 times larger than observed by KR. These two comparisons are the

only measure of  $R$  available, but both suggest that the  $R$  values are reasonable. The actual values of  $N_d \sim 10^9$  dislocations/cm<sup>2</sup>, as with values of  $R$ , are simply the result of the calculation employed here.  $N_d$  may be compared to the dislocation density due to plastic flow in alkali halides, which rarely exceeds  $4 \times 10^7$  dislocations/cm<sup>2</sup>.<sup>35,36</sup> It has been pointed out that the theory used here to describe  $\tau_D^{-1}$  does in many instances give values of  $N_d$  from thermal-conductivity fits which are 100 times the values obtained independently from etch pit counting.<sup>36,37</sup> The use of a theoretical calculation of  $\tau_D^{-1}$  by Ohashi<sup>38</sup> would give  $N_d$  15 times smaller than those reported here which is more in line with likely dislocation concentrations. Theories which invoke phonon interaction with mobile dislocations would not apply. In this case, unless the resonance of the interaction were above the conductivity peak, it would increase the temperature dependence to a higher power than  $T^3$  which is not observed. It is not likely that such a high-temperature resonance exists.

#### IV. CONCLUSION

The results reported here agree reasonably well with other recent data on the thermal conductivity

of solid neon. They also add new data at smaller molar volumes. We have measured the dependence of the conductivity on molar volume in the temperature range in which intrinsic scattering is dominant. A Callaway analysis shows that  $\tau_N^{-1} \propto \chi^2 T^4$  and  $\tau_U^{-1} \propto \chi^2 T^5 e^{-\Theta/6.5T}$  represent the natural neon data best. These results indicate that both Normal and Umklapp scattering processes are important. The analysis also showed that the mass defect scattering was enhanced by zero-point motion, and that this enhancement decreased with decreasing molar volume. Callaway fits to data from isotopically purified neon were markedly less successful than fits to natural neon. This leaves a large uncertainty in the value of  $B_N$ , which is shown to be volume dependent as well. It is hoped that these results may encourage a reexamination of more fundamental calculations of the thermal conductivity of solid neon.

#### ACKNOWLEDGMENT

The author wishes to express special thanks to M. V. Klein for his guidance in this investigation and his helpful criticisms of this manuscript.

\*Work supported by Advanced Research Projects Agency under contract No. DAHC-15-73-G-10 and the NSF under Grants Nos. GH-33634 and GH-37757.

†Based on a thesis submitted to the University of Illinois at Champaign-Urbana in partial fulfillment of the requirements of the Ph.D. degree. Present address: Dept. of Materials Science and Engineering, Cornell University, Ithaca, N. Y. 14853.

<sup>1</sup>G. Leibfried and E. Schlömann, *Nachr. Akad. Wiss. Goett. Math.-Phys. Kl.* **4**, 71 (1954).

<sup>2</sup>J. M. Ziman, *Electrons and Phonons* (Oxford U. P., Oxford, 1960), pp. 288-333.

<sup>3</sup>D. B. Benin, *Phys. Rev. B* **5**, 2344 (1972).

<sup>4</sup>C. L. Julian, *Phys. Rev.* **137**, 128 (1965).

<sup>5</sup>D. B. Benin, *Phys. Rev. Lett.* **20**, 1352 (1968); Ph.D. thesis (University of Rochester, 1967) (unpublished).

<sup>6</sup>B. J. Bennett, *Solid State Commun.* **8**, 65 (1970).

<sup>7</sup>D. K. Christen and G. L. Pollack, *Phys. Rev. B* **12**, 3380 (1975).

<sup>8</sup>D. B. Benin, *Phys. Rev. B* **1**, 2777 (1970).

<sup>9</sup>G. K. White and S. B. Woods, *Philos. Mag.* **3**, 785 (1958).

<sup>10</sup>R. M. Kimber and S. J. Rogers, *J. Phys. C* **6**, 2279 (1973).

<sup>11</sup>M. S. Anderson, R. Q. Fugate, and C. A. Swenson, *J. Low. Temp. Phys.* **10**, 345 (1973).

<sup>12</sup>F. Clayton and D. N. Batchelder, *J. Phys. C* **6**, 1212 (1973).

<sup>13</sup>I. N. Krupskii and V. G. Manzhelii, *Phys. Status Solidi* **24**, K53 (1967); and *Zh. Eksp. Teor. Fiz.* **55**, 2075 (1968) [*Sov. Phys.-JETP* **28**, 1097 (1969)].

<sup>14</sup>G. L. Pollack, *Rev. Mod. Phys.* **36**, 748 (1964).

<sup>15</sup>J. Callaway, *Phys. Rev.* **113**, 1046 (1959).

<sup>16</sup>C. Herring, *Phys. Rev.* **95**, 954 (1954).

<sup>17</sup>R. Q. Fugate and C. A. Swenson, *J. Low. Temp. Phys.* **10**, 317 (1973).

<sup>18</sup>P. Carruthers, *Rev. Mod. Phys.* **33**, 92 (1961).

<sup>19</sup>R. Berman, C. L. Bounds, and S. J. Rogers, *Proc. R. Soc. A* **289**, 66 (1965).

<sup>20</sup>R. Berman and J. C. F. Brock, *Proc. R. Soc. A* **289**, 46 (1965).

<sup>21</sup>J. A. Leake, W. B. Daniels, J. Skalyo, Jr., B. C. Frazer, and G. Shirane, *Phys. Rev.* **181**, 1251 (1969).

<sup>22</sup>J. E. Clemons, Ph.D. thesis (University of Illinois at Champaign-Urbana, 1975) (unpublished).

<sup>23</sup>H. D. Jones, Ph.D. thesis (Cornell University, 1968) (unpublished).

<sup>24</sup>Peierls's work is developed further by Ref. 2; R. Peierls, *Ann. Phys. (Leipz.)* **3**, 1055 (1929).

<sup>25</sup>S. C. Fain, Jr., and D. Lazarus, *Phys. Rev. A* **1**, 1460 (1970); W. D. Seward, D. Lazarus, and S. C. Fain, Jr., *Phys. Rev.* **178**, 345 (1969).

<sup>26</sup>P. G. Klemens, *Proc. Phys. Soc. Lond. A* **68**, 1113 (1955).

<sup>27</sup>P. G. Klemens, and A. A. Maradudin, *Phys. Rev.* **123**, 804 (1961).



<sup>28</sup>H. D. Jones, *Phys. Rev. A* 1, 71 (1970).

<sup>29</sup>R. D. Nelson and W. M. Hartmann, *Phys. Rev. Lett.* 28, 1261 (1972).

<sup>30</sup>D. T. Lawson and H. A. Fairbank, *J. Low Temp. Phys.* 11, 363 (1973).

<sup>31</sup>H. B. Casimir, *Physica* 5, 495 (1938).

<sup>32</sup>P. G. Klemens, in *Solid State Physics*, edited by F. Seitz and D. Turnbull (Academic, New York, 1958), Vol. 7, pp. 1-98.

<sup>33</sup>R. Berman, *Adv. Phys.* 2, 103 (1953).

<sup>34</sup>M. W. Ackerman, *Phys. Rev. B* 5, 2751 (1972).

<sup>35</sup>R. L. Sroull, M. Moss, and H. Weinstock, *J. Appl. Phys.* 30, 334 (1959); A. Taylor, H. R. Albers, and R. O. Pohl, *ibid.* 36, 2270 (1965).

<sup>36</sup>A. C. Anderson, and M. E. Malinowski, *Phys. Rev. B* 5, 3199 (1972).

<sup>37</sup>M. Moss, *J. Appl. Phys.* 37, 4168 (1966).

<sup>38</sup>K. Ohashi, *J. Phys. Soc. Jpn.* 24, 437 (1968).